Naval Research Laboratory

Washington, DC 20375-5320

NRL/MR/7210--06-9018

Design Considerations for the Second-Generation NPOI Fringe Tracker and Science Beam Combiner

XIAOLEI ZHANG
TOM ARMSTRONG
SERGIO RESTAINO

Radio, IR, and Optical Sensors Branch
Remote Sensing Division

DAVE MOZURKEWICH

Seabrook Engineering
Seabrook, Maryland

December 18, 2006

Approved for public release; distribution is unlimited.

REPORT DOCUMENTATION PAGE

Form Approved
OMB No. 0704-0188

Public reporting burden for this collection of information is estimated to average 1 hour per response, including the time for reviewing instructions, searching existing data sources, gathering and maintaining the data needed, and completing and reviewing this collection of information. Send comments regarding this burden estimate or any other aspect of this collection of information, including suggestions for reducing this burden to Department of Defense, Washington Headquarters Services, Directorate for Information Operations and Reports (0704-0188), 1215 Jefferson Davis Highway, Suite 1204, Arlington, VA 22202-4302. Respondents should be aware that notwithstanding any other provision of law, no person shall be subject to any penalty for failing to comply with a collection of information if it does not display a currently valid OMB control number. **PLEASE DO NOT RETURN YOUR FORM TO THE ABOVE ADDRESS.**

1. REPORT DATE *(DD-MM-YYYY)*	**2. REPORT TYPE**	**3. DATES COVERED** *(From - To)*
18-12-2006	Memorandum Report	

4. TITLE AND SUBTITLE

Design Considerations for the Second-Generation NPOI Fringe Tracker and Science Beam Combiner

5a. CONTRACT NUMBER

5b. GRANT NUMBER

5c. PROGRAM ELEMENT NUMBER

6. AUTHOR(S)

Xiaolei Zhang, Tom Armstrong, Dave Mozurkewich,* and Sergio Restaino

5d. PROJECT NUMBER

5e. TASK NUMBER

5f. WORK UNIT NUMBER

7. PERFORMING ORGANIZATION NAME(S) AND ADDRESS(ES)

Naval Research Laboratory
4555 Overlook Avenue, SW
Washington, DC 20375-5320

8. PERFORMING ORGANIZATION REPORT NUMBER

NRL/MR/7210--06-9018

9. SPONSORING / MONITORING AGENCY NAME(S) AND ADDRESS(ES)

10. SPONSOR / MONITOR'S ACRONYM(S)

11. SPONSOR / MONITOR'S REPORT NUMBER(S)

12. DISTRIBUTION / AVAILABILITY STATEMENT

Approved for public release; distribution is unlimited.

13. SUPPLEMENTARY NOTES

*Seabrook Engineering, 9310 Dubarry Ave., Seabrook, MD 20706

14. ABSTRACT

We describe the motivations for and the conceptual design of the second-generation back-end beam combiner and fringe tracker for the Navy Prototype Optical Interferometer. The new back end is expected to result in much-improved data quality and sensitivity compared to the existing back end. It will also enable the observations of geostationary satellites in the visible and near infrared regions of the spectrum.

15. SUBJECT TERMS

Optical interferometry Infrared interferometry
Satellite imaging

16. SECURITY CLASSIFICATION OF:			**17. LIMITATION OF ABSTRACT**	**18. NUMBER OF PAGES**	**19a. NAME OF RESPONSIBLE PERSON**
					Xiaolei Zhang
a. REPORT	**b. ABSTRACT**	**c. THIS PAGE**	UL	30	**19b. TELEPHONE NUMBER** *(include area code)*
Unclassified	Unclassified	Unclassified			(202) 404-2389

CONTENTS

1 Background 1

2 Conceptual Design 3

2.1 Top Level Design Considerations 3
2.2 Sensitivity Calculations 4
2.3 Possible Observing Configurations 5
2.4 Architecture of the Subsystems of the Beam Combiner 8

3 Fringe-Tracker and Science Beam Combiner Testbed 14

3.1 Specialty Components 17
3.2 Preliminary Procurement List 21

4 Software, Control System, and Interfacing with the Existing Instrument 23

5 Potential Impact 25

6 References 25

1 Background

The existing beam combiner/fringe tracker (Mozurkewich 1996) on the Navy Prototype Optical Interferometer (NPOI, Armstrong et al. 1998) has a mainly free-space, Michelson-type design (Figure 1). It produces interfered outputs of the six input beams on three spectrometers, and each spectrometer can accommodate up to four different baselines. Fringe-tracking signals and science data are produced simultaneously on the three spectrometers. It is a hybrid beam combination scheme incorporating features of both the pair-wise and the all-in-one beam combination schemes.

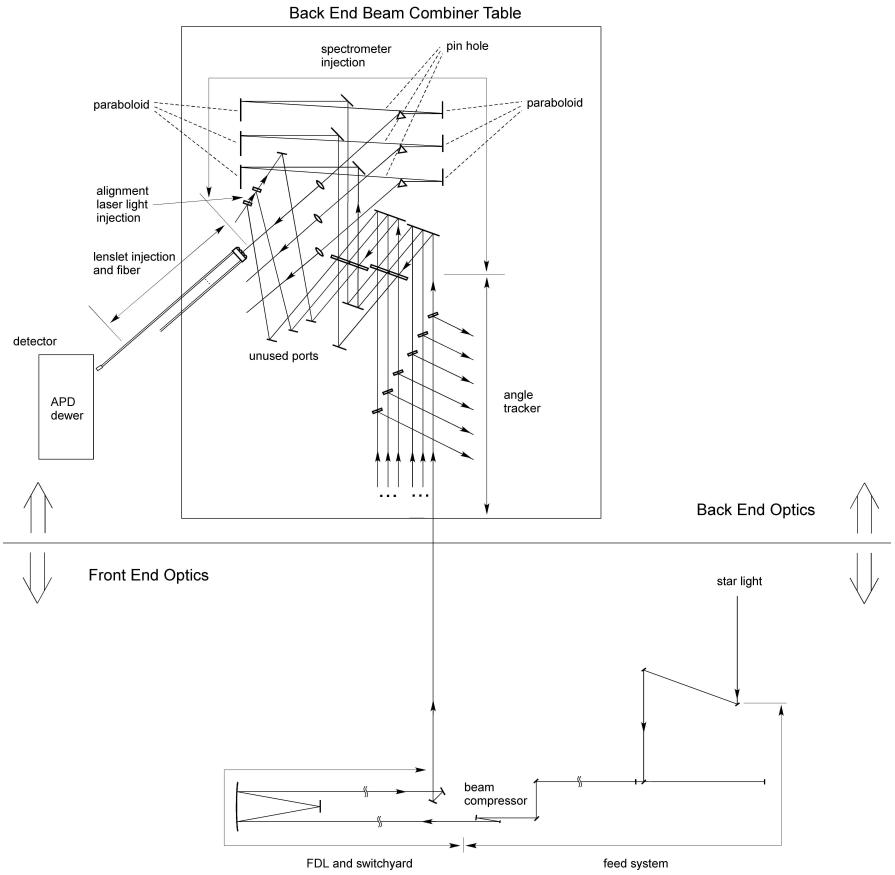

Figure 1: Current NPOI Optical Layout Showing the Front-End and Back-End Optics (Not to Scale)

The existing back end beam combiner has performed successful astronomical observations since its commission several years ago. However, certain

Manuscript approved October 16, 2006.

weaknesses of the this design also became apparent over time. First of all, due to the nonlinearity of the delay-line strokes and the nonlinear response of the Avalanche Photo Diode (APD) detectors, the fringes corresponding to the different baselines become entangled in the frequency domain when multiple baselines are placed on a single spectrometer, which gives crosstalk of signals among the baselines. It is desirable to replace the current beam combination scheme with one which is less vulnerable to component imperfections. Secondly, the APD detectors themselves are found to have afterpulsing issues in addition to nonlinearity, complicating data calibration and analysis. It is desirable to replace the APD detectors with the state-of-the-art CCD (charge coupled device) detectors which have large format, high quantum efficiency, fast readout speed and low readout noise. This, however, will mean to replace the current fringe-sensing scheme with one that does not involve the high-speed dithering of the delay-lines, so that the data readout speed is compatible with the CCD readout speed. Thirdly, the current scheme of obtaining the fringe tracking signal and science output using the same beam combination setup results in less flexibility in configuration according to stellar brightness and the choice of baselines. It is desirable to separate fringe tracking channel from the science channel, so that the optimum configuration for each application can be realized. Fourth, the current beam combiner has not implemented an adequate spatially-filtered photometric channel for the optimum calibration of data, especially those data which are intended for coherent integration. Fifth, due to the recent consideration of expanding NPOI's are of application to the imaging of geostationary artificial satellites, we need to re-evaluate the design requirements placed on the new beam combiner for this new application, including the incorporation of interferometric imaging in the near infrared (NIR) regime, as well as the larger flux level and spatial filtering requirement of the new 1.4 meter big telescopes.

These considerations prompted us to look into a new design of the beam combiner which incorporates the above-mentioned features. Since the current free-space beam combiner is being used to perform the day-to-day astronomical observations, and it is crucial not to let the future upgrade interrupt the daily operations of the working instrument, we plan to devise a stand-alone system which can be operated in parallel with the existing back end and also make use of the available real estate resources in the inner room.

2 Conceptual Design

2.1 Top Level Design Considerations

At the outset, we intend to choose a conceptual design for the beam combiner and fringe tracker which has the following characteristics:

- Separated fringe-tracking beam combiner and science beam combiner, so as to maximize the flexibility in optimizing the performance of each in terms of the choice of flux splitting ratio, integration time, as well as the choice of the subset of beams to interfere. We note that the fringe tracker could dub as a separate science beam combiner as well for certain type of astronomical observations: more discussions on this will be given later in the text.
- Spatial filtering and photometry calibration capabilities, so as to improve the precision we can achieve for the calibration of data.
- A separate NIR detection system dedicated to the satellite imaging applications, which will be used in conjunction with the visible-light fringe-tracking and science combiner during satellite observations.
- Use of CCDs instead of APDs as detectors for fringe-tracking and astronomical science applications, and eliminate high-frequency dithering from the delay-line servo.
- Allow maximum number baselines to be observed simultaneously, allow maximum closure-phase information in the science data.
- Stable operation and easy reconfiguration.
- Can be operated in parallel with the existing beam combiner. The control system for the new back end can be interfaced smoothly with the existing control software at the site.
- Allow further upgrades in the future as new technologies such as integrated optics in the visible and NIR wavelengths, etc., become available and mature.

2.2 Sensitivity Calculations

We first perform sensitivity calculations using the existing siderostats, and for astronomical sources (i.e. stars). This will be followed by estimations of satellite imaging using future 1.4 meter telescope with adaptive optics (AO) correction of wavefront.

Following Monnier (2003), we assume that a reasonable limit of detection (for fringe tracking, for example) is 10 photons per coherent volume per bandwidth of detection. Here the coherent volume is defined as the product of $r_0 \times r_0 \times t_0$, where the coherent length $r_0 = 10cm$, and the coherent length $t_0 = 10ms$. We use Vega's flux scale of $f_{vega} = 3 \times 10^{-5} erg \cdot cm^{-2} s^{-1}$, and its magnitude $m_{vega} = 0.05$, we obtained that for a 14th magnitude star (assuming unresolved),

$$-2.5 \log_{10} \frac{f_{star}}{3.e{-}5} = 14 - 0.05, \tag{1}$$

or

$$f_{star} = 8 \times 10^{-11} erg/cm^2/sec. \tag{2}$$

For a central wavelength of 550 nm, the above energy flux level can be converted to an approximate photon flux of

$$\begin{aligned} f_{star}(photon) &= 22\ photons/cm^2/sec \\ &= 22\ photons/(10cm)^2/(10ms). \end{aligned} \tag{3}$$

A partially-resolved source would reduce this number to about 10.

The above calculation assumed we receive all the photons in the visible bandwidth and for 100% throughput. For fringe tracking, assuming an effective bandwidth of 100 nm, and a system throughput of 2%, as are appropriate for NPOI, this corresponds to a magnitude reduction of 6. So the actual observational magnitude limit for the current system should be about 8. In reality, our experience showed that the actual observation magnitude limit is about 6, taking into account other imperfections of the system such as angle tracking.

A geostationary satellite is often found to be in the visible magnitude range of 9 to 15, from ground-based observations using single-aperture optical

telescopes of 20-30 inch class (most of results of the amateur observations of the geostationary satellites using single-aperture optical telescopes can be found on the World Wide Web). With the expected addition of the 1.4 meter telescopes fitted with adaptive optics into the NPOI system, we expect a significant improvement in sensitivity, although the quantitative performance of the AO with these bigger telescopes is at the moment still an unknown. Assuming the AO could extend the coherent aperture from 10 cm x 10 cm, which is what we used in the above calculations, to about 50 cm x 50 cm (for 1.4 meter telescope, this corresponds to a Strehl ratio of about 16%), i.e., a factor of 25 improvement in collecting area, we would be gaining 3.5 magnitude in detection limit (i.e. to magnitude 9.5), already into the range where we can observe the brightest of the artificial satellite (during some brief period of glinting when the satellite reflect sunlight in the most favorable angle to the earth, its effective magnitude could reach to about 7-8). Further improvement in AO performance will extend this magnitude limit even further, especially if coupled with the improved performance of the optical throughput of the back end beam combiner, and the increased bandwidth offered by the combined visible and NIR detection channels. We show in Figure 2 an expected spectral distribution of the satellite signal assuming it acts as a passive reflection of the solar light.

2.3 Possible Observing Configurations

A schematic layout of the new back end in block diagram form is given in Figure 3. The light that will be intercepted from the beam propagation path of the exist NPOI optical train will be just after the beam compressor (c.f. Figure 1). A Risley prism on each beam line will correct for the lateral dispersion caused by the atmospheric differential refraction (Zhang 2002), which is especially important for low-elevation satellite observations. Part of the light will be directed by six beam splitters to determine the slow-varying angle tracking signals (with the high-bandwidth compensation performed by the AO system of the big telescopes when they are in use, or by the current narrow angle tracker (NAT) system if we use the existing siderostats), which adjust the coupling to the spatial-filtering single-mode fibers (these will likely be the so-called "endless-single-mode" photonic crystal fibers, which can si-

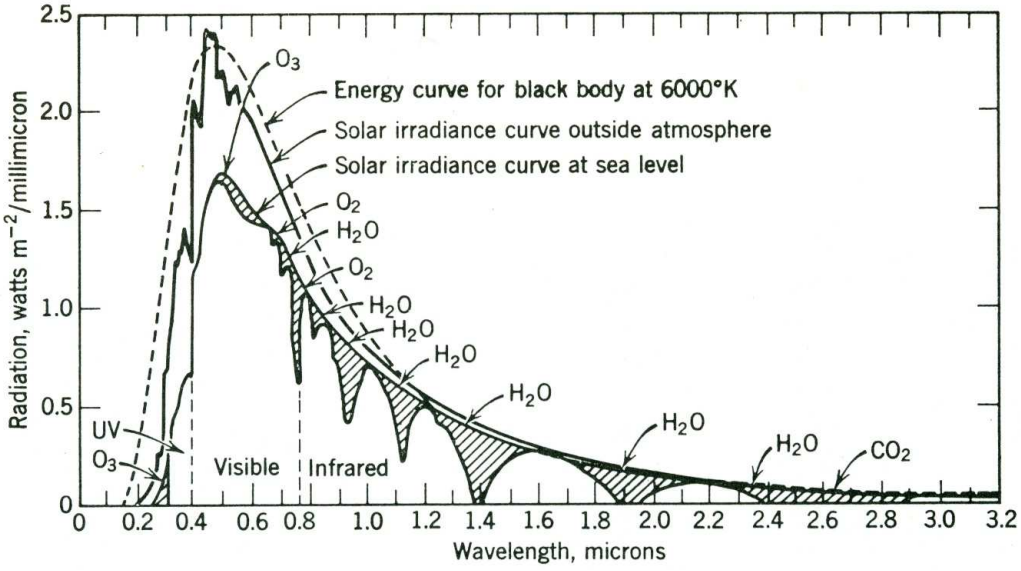

Figure 2: Spectrum of the Sun in the Visible and IR Range (from Handbook of Geophysics)

multaneous admit both the visible and NIR light. See further discussion later). This is followed by a set of six dichroic beam splitters which separate the light for the visible and NIR beam combinations. The dividing wavelength for visible and NIR channels is currently planned as 900 μm.

The visible light is further split by a set of polarizing beam splitters, and one of the channels is used for fringe tracking, and the other channel for science beam combination. Note that here we indicated the option of swapping the beam splitters (BS) with mirrors, or swapping the BS/mirrors out so that all the visible light can go to either the science beam combiner, or to the visible-light fringe tracker. This anticipates the possibility that for certain S/N-critical observations, we might want to either use NIR light to do the tracking, and all the visible light for science beam combination (as for certain stellar imaging observations), or else send all the visible light to the visible-light fringe tracker (as in the satellite observations).

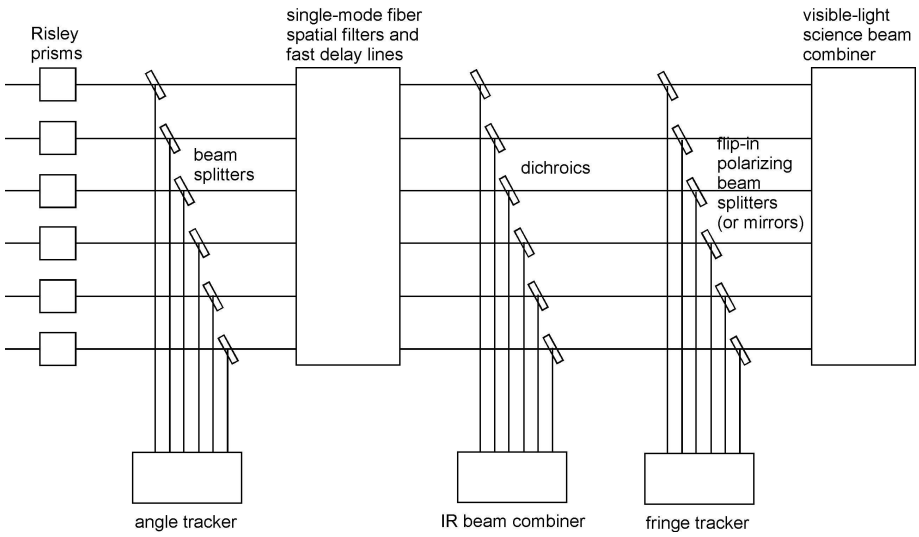

Figure 3: Block Diagram of the NPOI New Backend

2.3.1 Usage of Fringe Sensor as a Stand-Alone Science Instrument

The fringe sensor is planned to be a pair-wise beam combiner. In a 6-way, non-redundant configuration, this implies that there will be 5 pairs of combined beams. Since in a pair-wise configuration one does not have to worry about cross-talk issues, we plan to use the fringe sensor unit also to do a portion of the science projects, i.e., that of parametric-measurement nature, such as stellar diameter measurements, limb-darkening measurements, etc., which require only the intensity information, and not the closure-phase information.

2.3.2 Usage of Science Beam Combiner in Conjunction with Fringe Sensor

The science beam combiner we currently envisioned is of an all-in-one type (see further the discussion in section 2.4.1). This combiner will be mainly used for imaging sources of high brightness so signal-to-noise (S/N) will be

less of an issue. The closure phase information will be obtained in this configuration. So is the possibility for coherent integration.

2.3.3 Satellite Imaging Considerations

As the sensitivity calculations in the previous section had shown, depending on the performance of the AO, we are of marginal sensitivity in being able to see the faintest of the geostationary satellites, thus the consideration of incorporating the photon flux from the NIR region of the spectral range as well as the visible region. Even though the solar spectrum has less intensity in the NIR region, since each photon is less energetic, the photon number flux in the NIR is still quite significant.

In terms of the angular sizes of the satellites, assuming that a standard satellite is of linear size of 3-5 meters, and the geostationary orbit is at a distance of 7.1×10^7 meters from the surface of the earth, the angular size of the satellites are between 8-15 mas, whereas the field-of-view of the 1.4 meter telescope is about 100 mas. So the satellites should observable by the NPOI with the 1.4 meter telescopes as far as the angular size of the satellites is concerned (currently the stellar observations are routinely done for stars of diameter 0.5-10 mas).

2.4 Architecture of the Subsystems of the Beam Combiner

To determine the detailed architecture of the subsystems of the new back end (the visible-light fringe tracker and science beam combiner, NIR beam combiner, and angle tracker), we have surveyed the existing technologies and layouts of the other ground-based optical interferometers, and made the initial choice based on the compatibility with the overall observing scheme as outlined in the last section, and on the availabilities of the necessary components including especially the detectors.

2.4.1 Visible-Light Science Beam Combiner with Photometric Calibration Channels

From the design studies carried out, and the initial experiences gained of the newest generation of ground-based optical interferometers such as CHARA and VLTI, we have decided to similarly pursue a science beam combiner in the so-called all-in-one configuration (Figure 4). This configuration has been used for CHARA's visible and IR science beam combiners (Ten Brummelaar 1994; Ridgeway 1994, Monnier et al. 2004). Using this scheme the input six beams of NPOI can be brought into a one-dimensional non-redundant array (but unlike CHARA, we will likely not to implement the science combiner with single-mode fibers, since the beam had already gone through the photonic fiber spatial filter once earlier in the optical train: see Figure 3), which are then focused by an achromat and two cylindrical lenses (or alternatively parabolic mirrors) of differing focal lengths onto an image plane where a CCD camera lies. A prism or grating will precede the imaging optics to expand the image spot into spectral bands in the focusing direction of the short focal length cylindrical lens. The fringes formed in the wider direction of the Airy pattern are Fourier-transformed to obtain the autocorrelation function of the exit-pupil one-dimensional array, which is used to determine the complex visibility functions corresponding to the different baselines.

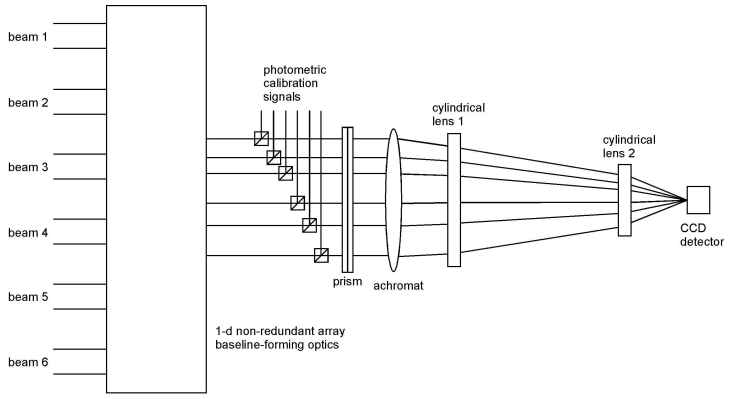

Figure 4: Schematics of the Six-Way, All-in-One Science Beam Combiner

If the photometric calibration signal is split off after the single-mode spa-

tial filtering, the intensity fluctuations in the photometric channel is found to track accurately the wavefront phase gradient in the science channel (Coude du Foresto 1997).

Using the free-space instead of fiber-based implementation of the all-in-one scheme does require one to pay special attention to the stability of the final baseline units. The potential crosstalk issue in the all-in-one combiner should also be explored and avoided.

During the initial design phase we have also considered the possibility of using a pair-wise fiber beam combination scheme for the science beam combiner, taking notice of the excellent calibration fidelity of the first generation VLTI instruments such as VINCI (Kervella et al. 2004), which utilizes the pair-wise combination scheme on their small number of input beams and over narrow operation band. However, we realize that due to the broad-band nature of the NPOI, as well as the fact that we have six input beams, to realize a pair-wise beam combiner for all the baselines would be prohibitively complicated and bulky (since we have 15 baselines total, each is likely to need to be sub-divided in frequency band in order to be used in a Michelson type of pair-wise fiber combiner, since fiber beam splitters are not yet available in the photonic crystal fibers version). This option can still be considered in the future generation of integrated optics beam combiners, which naturally reduces the sizes of the components.

2.4.2 Fringe Tracker

A fringe sensor/tracker used in optical interferometry generally involves a spectral-dispersion unit for group-delay tracking, and a phase-shifting or phase-stepping unit for fringe parameter determination. Following the current practice on NPOI (Benson, Mozurkewich, & Jefferies 1998), we intend to integrate the two tasks into the same instrument, by introducing spectral dispersion into the phase-stepped outputs. We need to explore the different options for the spectral dispersing element, though the 60-degree BK7 glass prism is known to result in uniform dispersion in κ space. Figure 5 shows the schematic layout of such a 6-way fringe tracker.

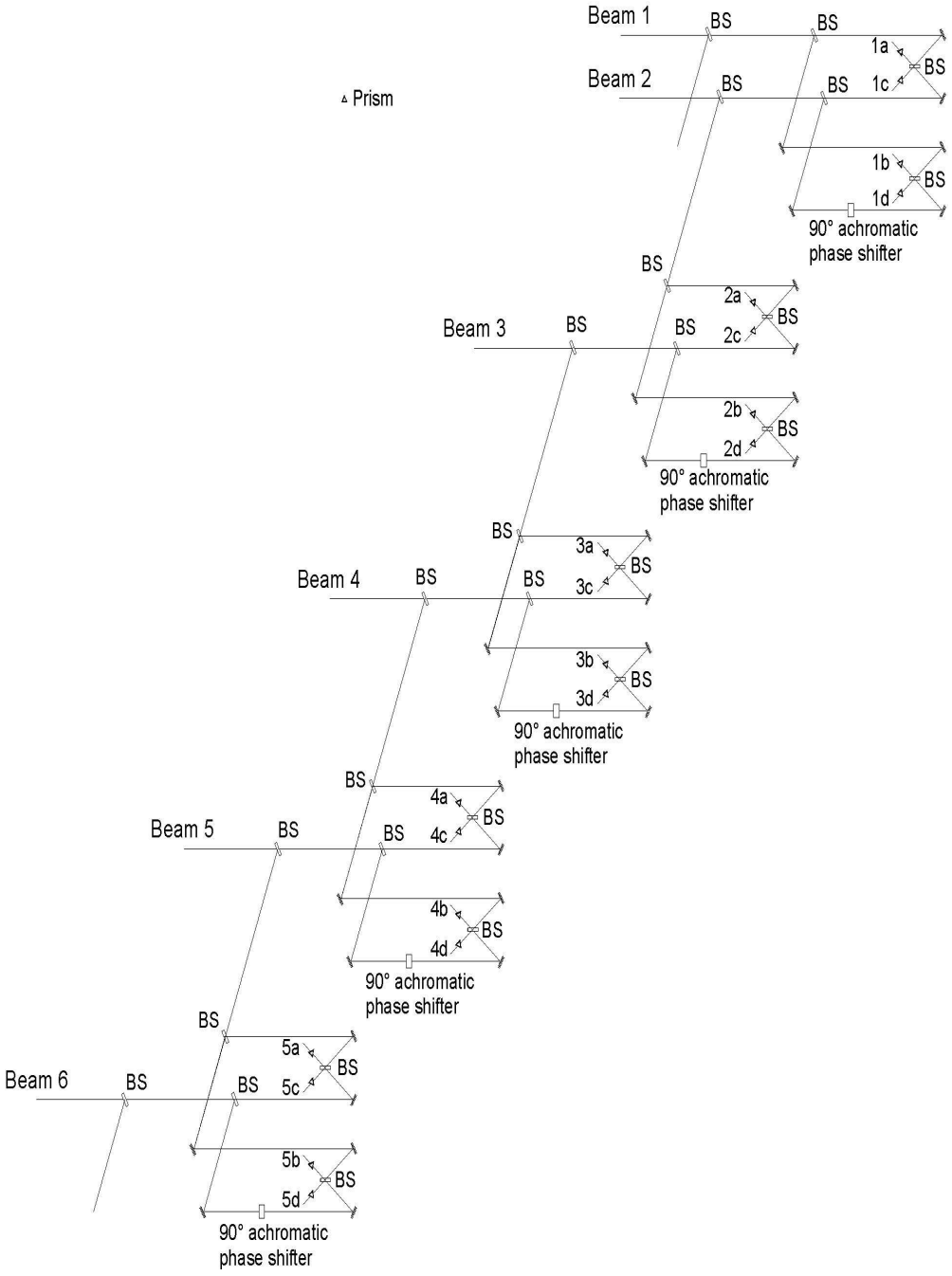

Figure 5: Schematic Layout of the Six-Way Quadrature-Type Fringe Sensor

Following Lawson (2000), if we perform measurements of A,B,C,D (which corresponds to intensity measurements of two interfering beams with phase-shift of zero, one, two and three quarters of waves) at a series of wavelength λ_m (or equivalently, wave number $\kappa_m = 1/\lambda_m$), with m = 0, 1, ... M-1, where M is the number of detector pixels in the dispersion direction, then

$$h_c(\kappa_m) = A(\kappa_m) - C(\kappa_m) \propto \cos(2\pi\kappa_m x) \quad m = 0, ..., M-1 \tag{4}$$

$$h_s(\kappa_m) = B(\kappa_m) - D(\kappa_m) \propto \sin(2\pi\kappa_m x) \quad m = 0, ..., M-1. \tag{5}$$

Let

$$h(\kappa_m) = h_c(\kappa_m) + j h_s(\kappa_m), \quad m = 0, ..., M-1, \tag{6}$$

Its discrete Fourier Transform $H(x)$ is

$$H(x) = \Sigma_{m=0}^{M-1} h(\kappa_m) \exp(j2\pi\kappa_m x) \tag{7}$$

where the peak in the $|H(x)|^2$ can be used to determine the group delay (and can be co-added between frames to increase signal-to-noise). The phase of the fringe can be determined from the ABCD quantities (Wyant 1975; Shao and Colavita 1992; Lawson 2000), and the usual phase closure procedure can be used to reduce the impact of station-based phase errors.

In considering the design options for the next-generation fringe tracker, especially on the ways for realizing the delay modulation for phase detection, we have been constrained by the desire to use CCDs as detectors for the visible-light region, which could alleviate the adverse performance characteristics of the APDs we had encountered so far. Due to the intrinsic low readout speed of the CCDs compared to the APDs, this choice means that we would no longer be able to use delay-dithering to realized the phase-stepping scheme for fringe parameter determination, as is currently implemented on the NPOI. Instead, we are planning to implement the four quarter-wave phase shifts by using an achromatic phase retarder, as well as mirror reflection (which introduces one-half wave phase change). A by-product of using a phase-stepping scheme such as the quarter-wave phase shifters instead of a phase-shifting scheme such as dithering is that one gains about another 10% in S/N.

The implementation of the fringe srnsor need to be done in free-space because of the need to insert the quarter-wave phase shifters into the beam path. This will be done after the initial wavefront clean-up by the single-mode fiber (Figure 3). At this point the re-collimated beams could be significantly reduced in size so the phase-shifting elements we choose to use could be small in physical size as well.

2.4.3 NIR Beam Combiner

The detailed design of the NIR beam combiner is yet to be carried out. We are likely to implement a pair-wise beam combination scheme of some sort, taking into account of the fact that we might want to implement a stand-alone NIR fringe tracker in addition to the visible-light fringe tracker.

2.4.4 Precision Angle Tracker

The existing angle tracker on the working instrument is likely not to be adequate for achieving the level of angle tracking stability needed for light injection into the single-mode optical fiber. Therefore additional angle sensing and servoing functionality will be required as part of the implementation of the new back end. We will here consider only the implementation of a low bandwidth, high-precision angle tracker, and leave the task of high-bandwidth tip/tilt correction to the AO system of the big telescope that are expected to be tested with the new back end.

The angle-sensing signals will be split off from the 6 beams before they is are sent to the fringe tracker and the IR and science beam combiners (Figure 3). Those latter paths will go through the same spatial filtering by short segments of single-mode fibers before they are further split off, so their phases are tied to one another.

Once again CCD camera and associated focusing optics can be used for imaging the 6 beam spots in order to derive the angle-tracking signals.

3 Fringe-Tracker and Science Beam Combiner Testbed

In order to validate design concepts and obtain the performance characteristics of the proposed approaches and implementation, we plan to construct a testbed at NRL in the upcoming years. The testbed is expected to be used to explore and test all aspects of the design. As a first step towards this goal, a prototype of a complete two-element fringe sensor system is planned to be constructed and used during the site-testing of the 1.4 meter telescopes. This system will also include rudimentary angle-tracking and spatial-filtering capabilities.

Figure 6 shows the schematic of a two-way fringe tracker we intend to construct during the testbed phase of the new beam combiner prototyping. In this plot we illustrated the implementation of an achromatic quarter-wave phase shifter through two types of glass (BK7 and Fused Silica). We have initially explored the use of only one type of glass to realize such a shifter. But these initial efforts show that the resulting phase plate designs do not meet the adequate bandwidth and practical realizability requirement.

Following Morgan, Burge, & Woolf (2000), we also considered the two-glass and air gap approach, and obtained a set of parameters that gives a fairly good achromatic quarter-wave phase shifting performance (Figure 7). Note that the resulting parameters for the glass and air-path thicknesses ($t_{air} = 51.218\mu m, t_{BK7} = 189.6\mu m, t_{FS} = -232.2\mu m$), are difficult to manufacture and to support mechanically if these thicknesses were made into a single piece of glass. Instead, they are expected to be realized as the thickness difference of two pieces of glass of the same material, placed on the two beam paths as shown in Figure 6. In the final design process the tolerance to angular tilt of the glass (used to achieve the precision thickness difference values) need to be studied incorporating the spectral dispersion of the glass refraction.

In Figure 8, we plot the performance of the above quanter wave plate under a thickness perturbation of 0.1 μm on the BK7 glass (which would corresponds to an angle perturbation of 22' if the BK7 glass is of thickness

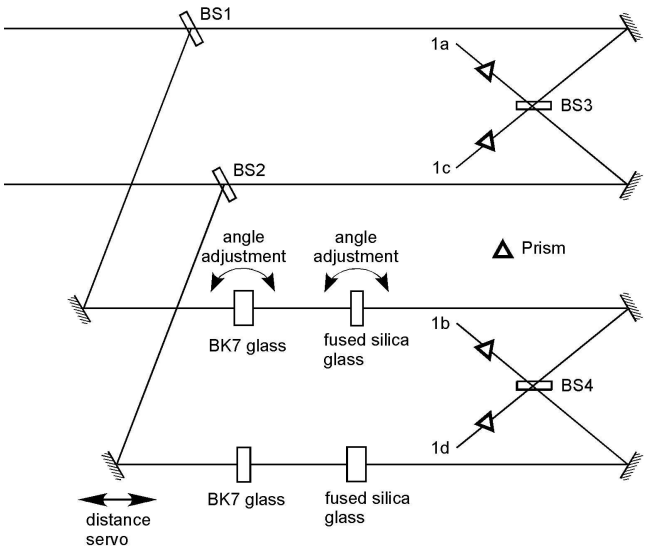

Figure 6: Schematics of the Two-Way Quadrature-Type Finger Tracker Using Two Types of Glass for Quarter-Wave Phase Shift and Prism for Spectral Dispersion

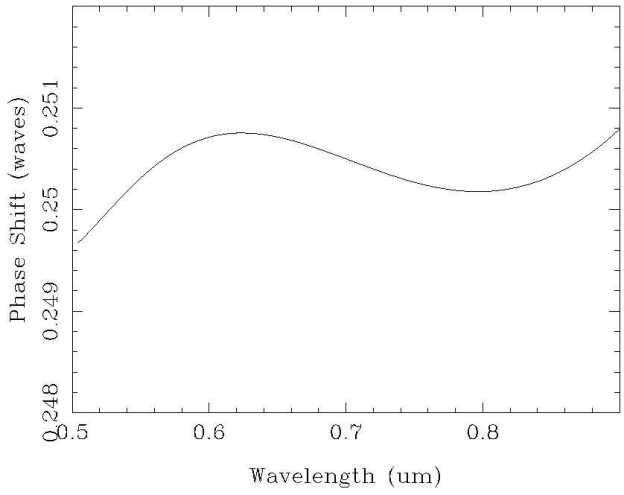

Figure 7: Performance of the Quarter Wave Plate Using BK7 and Fused Silica Plus Air Path, at Design Parameters

of 5 mm), and a compensating thickness reduction in the airpath of 0.152 μm. It is seen that once again the performance is acceptable as long as the airpath is adjusted accordingly. Without this adjustment (i.e., if the angle simply tilt by this much, which gives a corresponding airpath decrease of 0.1 μm), the phase shift would change from close to 0.25 wave to that of 0.31 wave, clearly not acceptable. Therefore, careful pathlength and occasional angle adjustment would be needed for this type of implementation of the achromatic quarter-wave phase shifter.

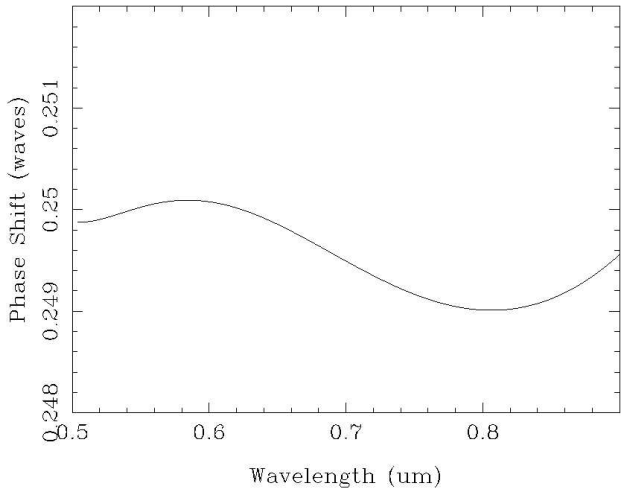

Figure 8: Performance of the Quarter Wave Plate Using BK7 and Fused Silica Plus Air Path, With or 0.1 μm Thickness Increase on the BK7 Glass, and a Compensating 0.152 μm Thickness Increase in the Air Path

Alternatively, in section 3.1.4 we will also explore various commercially available achromatic quarter-wave retarders. Some of these will be tested on the testbed as well, and potentially these could simplify the implementation and operation complexities of the fringe tracker considerably, especially if we were to use it in the six-way mode in the future (Figure 5). We will need to pay close attention to the throughput issue since some of these alternative achromatic phase shifters could be quite lossy.

In addition to testing the fringe sensor/tracker design and implementation, the testbed will allow us to learn the performance of single mode fibers,

in particular the photonic crystal fibers, their coupling efficiency, sensitivity to stress, as well as alignment tolerances. We will also devise an effective sensing and feedback mechanism for the closed loop servo control of fiber coupling. The detected fringe signal on the testbed will allow us to assess the S/N needed for effective fringe detection during astronomical observations, and thus what magnitude range of stars are best suited for imaging, as well as to extrapolate to the performance of satellite observations, and compare our finding with previous calculations such as that of Ten Brummelaar (1995) and Millan-Gabet et al (1995).

As a second stage of the testbed work, a 6-way science beam combiner will be implemented (Figure 4). Using it we will explore the best approach of utilizing the photometric calibration signals, as well as determine what CCD bit depth/readout rate combination serves as the best choice. We will explore and prevent potential crosstalk issues between the different spatial frequencies, though the old problems of the nonlinearities in the APD detectors and in the delay-dithering scheme will no longer be there. Further down the line we also plan to implement the NIR beam combination capabilities.

3.1 Specialty Components

In this section we give some more details of the choices and properties of several specialty components used in the critical parts of the new back end beam combiner.

3.1.1 Photonic Crystal Fibers

Since in the visible range the available single mode fibers are mostly only 100 nm in bandwidth, and the single-mode range of fiber beam splitters is even narrower, we have decided to test the use of photonic crystal fibers (see, e.g., Peyrilloux, Pagnoux, & Reynaud 2003), in the so-called "endless single mode" regime, which can result in the effective single mode range from 300nm to 2μm. The drawbacks with the photonic crystal fibers are their high propagation loss, high cost, and sensitivity of their spectral response to bend-

ing stress. These can be circumvented by using only short segments of the photonic crystal fibers (i.e., less that 1 meter in length), and adopting careful mounting scheme. Another issue related to the use of photonic crystal fibers is the variation of numerical aperture with wavelength, due to the variation of the mode shape in the photonic crystal fiber with wavelength. If we want to handle the entire visible waveband by a single piece of fiber, we will need to tolerate further coupling loss at the edges of the band, or develop clever nearly frequency-independent coupling optics (one of the possible implementation of the latter is currently under investigation). Polarization-preserving versions of the photonic crystal fibers are also available.

We will explore the dispersion-balancing characteristics of certain photonic crystal fibers, as a flat dispersion curve can relax the requirement of length-matching for the six fiber segments used to transport the six beams, and they would resemble more the current vacuum fast delay lines (FDLs). The residual dispersion introduced will need to be determined and factored into the analysis for fringe parameter determination.

One Dutch company, Crystal Fibre, makes the polarization maintaining endless-single-mode photonic crystal fibers that cover the visible and NIR wave band. These fibers are expected to be stretchable like conventional fibers so they can be used to realize a stand-alone FDL system. A typical free space coupling efficiency of such fibers is around 75% according to the company, using a single aspheric lense.

3.1.2 CCDs for Visible Band Observations

The CCD cameras used for fringe sensing, angle sensing, and science beam combination in the visible-light range are ideally preferred to be of high quantum efficiency (QE, preferably close to 1), high frame rate (preferably close to 1kHz frame rate for a 100x100 pixel area CCD), and low read noise (ideally close to or less than 1 per pixel), and of affordable price. At the moment, these characteristics could not all be satisfied with the same model of CCD available on the market. Our choice, for the testbed and for the different generations of actual instruments, will be made as a best compromise of our

objectives and available resources.

One possible choice is the SamBa series of cameras from Sensovation (a Germany company with US sales office in CA). Among them the Samba SE-34 model can provide up to 1 kHz frame rate if we sub-window it to 100x100 pixels on the lower-left corner of the acquisition window. It has 1e readnoise, negligible dark noise at 1kHz frame rate, but only 40% peak QE. It costs about 11 K each, which is relatively affordable compared to other cameras of similar characteristics.

Another possible choice of the CCD is the Marconi/E2V I3CCD. A small format version (L3Vision CCD60) has a 128x128 format, 1 kHz frame rate (or 11 MHz data rate), less than 1e read noise, and 90% peak QE. The cost is about $34K. Apart from the high cost, this camera also has large heat dissipation rate. Also, to achieve the ultimate limit of a few electron per frame of read noise, the camera needs to be cooled to liquid Nitrogen temperature (which is not practical for on-site observation at Flagstaff either with the construction of a closed-cycle system, or else with the boil-off of portable LN sources), although the $\sim$ 1e read noise per pixel can be achieved with TE cooling alone.

3.1.3 NIR Array Detectors

In order to perform satellite imaging at NIR wavelengths as well, we need to look into the available characteristics and costs of the NIR array cameras. The best IR cameras in the US are manufactured by two companies, Sensors Unlimited and FLIR/Indigo System.

The Sensors Unlimited offers two models of IR cameras covering he wave-band from 900nm to 1700 nm. The MX model has 50 e read noise but is capable of a frame rate of only 60fps. It costs about 24K each. The MSW model has 400 e read noise, but can do sub-windowing with extremely high frame rate (more than we will need at the 1kHz). Its QE is about 60%. It costs about 28K each.

FLIR/Indigo System has released a new series of IR cameras (SC-6000HS)

with InGaAs FPA detector array. Among these the sub-model SC-6000HS-NIR has characteristics quite close to what we will need. The camera has 640x512 pixels as well as has subwindowing capability. Thus with its 50Mhz data rate, it provides a frame rate more than meeting our specs. The read noise is about 65e for low gain mode and 530e for high gain mode. The peak QE is about 65%, though on these latter two characteristics the company had not given a quantitative quotation of the performance characteristics. The cost is around $73K, significantly more than the Sensors Unlimited models.

Both of these companies also provide a model of NIR camera that covers the visible waveband simultaneously, with additional cost. Since we have decided to divide the visible and IR portion of the band, we will not look into this option.

3.1.4 Achromatic Quarter Wave Phase Retarders

Due to the complication and cost-concerns of implementing the 4 pieces of glass-plate achromatic phase shifters per baseline, we have also looked into commercially-available achromatic quarter wave phase retarders. One version of it was made according to an approach developed by Pancharatnam (1955), sold by the German company Bernhard Halle Nachfolger GmbH. It is made with Mica and has a peak wavefront error less than 0.01 wave in the entire 400nm to 800nm waveband, but has a throughput loss of nearly 50%. The cost for an 1 inch aperture version is about 1365 Euro. Another version (also sold by the same company as the Mica retarders) is made with quartz/MgF_2 (Serkowsky 1976; Frecker & Serkowsky 1976). In the so-called Superachromatic version, the quartz/MgF2 retarder each consists of three pairs of quartz and MgF_2 and a peak path difference of 0.01 wave in the 310-1100nm range. The cost for a 1 inch aperture plate is 7365 Euro. The quartz/MgF_2 phase retarder is expected to have significantly less loss than the Mica phase retarder.

There is another type of achromatic phase shifter called Fresnel Rhomb (see, e.g. Hecht 1998), which accomplish achromatic phase shifting through the different phase changes on internal reflection of the p and s components

of an incident plane polarized beam. Fresnel rhombs can be manufactured in BK7 glass for 365nm-900nm application. This product is sold by many companies including a British company Halbo Optics. The price is between 1000-2000 pounds for a quarter-wave phase retarder. The Fresnel Rhomb phase retarder has excellent achromatic characteristics (about 1 degree of phase shift over the visible band) and negligible loss. It however does involve the need to deal with a lateral shift of beam axis between the input and output beams. Also there is the issue of the resulting wavefront quality.

3.1.5 Fiber Stretchers

Utilizing optical fiber stretcher to implement optical delay lines has become a routine practice (Furstenau & Schmidt 1990; Reynaud & Delaire 1994; Henderson et al. 2004). According to these references we could obtain about 1.1 mm stretching range with 5 meter fiber length. This entire range is only needed for the initial test when we want the fiber stretcher to cover the entire automated FDL pathlength compensation range so we can have a stand-alone fiber delayline system, after dialing the rough delayline setting for the current FDL for each source at a given time. In the future for final integration of the new bac kend we can have FDL do part of the pathlength compensation, therefore the length of photonic fiber needed could be reduced if the loss of it is a concern.

We have identified a Canadian company which manufactures fiber stretchers, Candian Instrumentation & Research Ltd. The cost of the stretcher and controller together is about 2000$, and we will need to provide the fiber segments to be installed onto the stretcher.

3.2 Preliminary Procurement List

In the following we listed the components needed for a 6-way science beam combiner and 6-way fringe tracker, as well as an angle tracker. The parts needed for the IR beam combiner will to be determined in the future. Initially, when implementing a 2-way fringe tracker in the lab, only a fraction

of the components listed below are needed.

```
Beam splitters:
  30 each (for quadrature fringe tracker)
  6 each (polarizing variety,
          for separating fringe tracking and science)
  6 each (for separating science and photometric calibration)
  6 each (for angle tracking)
  6 each (dichroic variety,
          for separating IR beam combiner with the visible beam combiner)

3-axis positioner system from Thorlabs for single-mode fibers.
Controller, stages, and electronics.
  6 sets

Fiber light-injection optics (lenses or paraboloids).

Photonic crystal fibers:
  6 each, 1 meter length
  2 each, 5 meter length

Fiber stretchers
  6 sets

CCD Sensovation AG SamBa SE-34, or CCD60 from Marcono/E2V
  6 each

We have available already 2 copies of CCD Adimec-1000m, which can be used
on the first testbed, in conjunction with an existing image-intensifier,
to be used for fringe tracking and angle tracking.

Baseline forming optics and relay optics for the science beam combiner
including cylindrical lenses/mirrors and prism/grating/grism.

Controller and translation stages for fringe-tracker glass path
  6 sets
```

```
Phase retarder optics and dispersion optics for the fringe tracker
  6 sets

Angle-tracker optics and mounts (initially not servoed)
  6 sets

Various  auxiliary optics.

Fast data recorder and computer
  several sets (depending on the final configuration) for science combiner
fringe tracker and angle tracker

Optics and detectors for the NIR combiner (TBD)
```

4 Software, Control System, and Interfacing with the Existing Instrument

The software used for image acquisition, high-speed data acquisition, and motion control is currently planned to be National Instrument (NI)'s LabWindows/CVI. This software package uses the same/or similar low-level instrument drivers as the more popular Labview software, they also produce similarly-looking graphical user interface. The functionalities these two softwares can perform are also comparable, though for the most time-critical applications the Labview-RT version of the software still has an edge. But instead of the circuit-diagram type of programming language used by Labview, the CVI uses standard C language, and it invokes instrument driver through functional calls. CVI has a fully object-oriented architecture, and it comes with a standard C-compiler and can incorporate user-implemented routines and external function libraries. It allows the implementation of functionalities such as DDE (direct data exchange) and DLL (dynamically linked libraries) for easy communication with applications created or running on other platforms. CVI has single-use license and it does not require renewal, the license is furthermore transferable among computers (as long as only one

computer is registered for the use of license at a time).

The CVI top-level codes usually interact with instruments with three kinds of instrument driver libraries: NI-IMAQ for image acquisition through an NI frame grabber board interfaced to a NI-compliant camera; NI-DAQ for high-speed analog and digital signal acquisition; NI-Motion for controlling NI motions controllers interfaced with NI-compliant motors and amplifiers. These driver libraries usually ship free with the NI boards and hardware one purchases, no separate licenses are required, although for more sophisticated image processing applications NI-Vision software is needed, which we are in the process of procuring.

CVI can be run either with Windows operating system, or on a Sun with unix operating system. NI-DAQ boards usually have internal clocks and timing pulses, which had a resolution/accuracy on the order of 2 μs. These on-board timing signal can be used to acquire time-critical fringe tracking and science signals, whereas the data writing into file can be accomplished asynchronously through the CVI ring buffer or parallel data buffer.

Furthermore, if, for example, we were to use the Thorlabs APT-series controllers, whose software interface is built on Active-X control, CVI is fully compatible with this architecture, and both support multi-threaded applications which allow asynchronous real-time capabilities mentioned above.

In interfacing with the existing software and control system at the site in the future, we will explore the DDE/DLL type of processes. Fortunately, for the stand-alone new back end envisioned, most of the fringe-sensing, fringe-tracking, data-recording tasks will be accomplished by the new stand-alone computer we will procure for the new back end (which might involve a high-speed data recorder for the science data recording), the current computer control system will serve to invoke the observing command, move the siderostats and delaylines to target, perform coarse angle tracking, and then signal to the new back end computer to perform the rest of the tasks.

5 Potential Impact

Apart from the prospect of obtaining a high performance science-beam-combiner, fringe-tracker and angle-tracker module for NPOI, which will significantly improve the data quality and calibration accuracy, the experience gained in this development may also benefit other new and prospective ground-based optical interferometers, such as VLTI, CHARA, MRO, as these are also intended to have a large number of input beams for the final instrument, and are also currently looking into the same kind of design options that we are studying. The imaging of geostationary satellite by optical interferometry will be the first ever such effort to be carried out and thus will break new ground in this area.

6 References

Armstrong, J.T., Mozurkewich, D., Rickard, L., Hutter, D.J., Benson, J.A., Bowers, P.F., Elias II, N.M., Hummel, C.A., Johnston, K.J., Buscher, D.F., Clark III, J.H., Ha, L., Ling, L.-C., White, N. W., & Simon, R.S. 1998, "The Navy Proto Type Optical Interferometer", The Astrophysical Journal, 496, 550

Benson, J.A., Mozurkewich, D., & Jefferies, S.M. 1998, "Active Optical Fringe Tracking at the NPOI", in Astronomical Interferometry, R.D. Reasenberg, ed., Proc. SPIE 3350, 493

Coude du Foresto, V. 1997, "Fringe Benefits: The Spatial Filtering Advantage of Single Mode Fibers", in Integrated Optics for Astronomical Interferometry, eds. P. Kern and F. Malbet, p.27

Frecker, J.E., & Serkowsky,K. 1976, "Linear Polarimeter with Rapid Modulation, Achromatic in the 0,3 - 1,1 m range" Applied Optics 15, p.605

Furstenau, N., & Schmidt, W. 1990, "Sensor Applications of a Fiberoptic Multistable Michelson Interferometer with Electrooptic Feedback", Fiber Optics Sensors IV, Proc. SPIE vol. 1267, p.105

Hecht, E. 1998, Optics (Reading MA: Addison Wesley Longman)

Henderson, D.A., Hoffman, C., Culhane, R. & Viggiano III, D. 2004, "Using Piezoelectric Actuation", Fiber Optic Sensor Technology and Application III, Proc. SPIT vol. 5589, p.99

Kervella, P. et al. 2004, "Optimal Interferometric Data Acquisition and Processing: Towards 0.1% Precision with the Single-Mode Beam Combiner VINCI", SPIE 5491, p. 741

Lawson, P. 2000, "Phase and Group Delay Estimation", in Principles of Long Baseline Interferometry, Michelson Summer School Lecture Notes, p. 113

Millan-Gabet, R., Schloerbm F.P., Traub, W.A., & Dyck, M.H. 1995, "Signal-To-Noise Ratio of Interference Fringe Parameters", IOTA Technical Report

Monnier, J.D. 2003, "Optical Interferometry in Astronomy", Rep. Prog. Phys., 66, 789

Monnier,J.D., Berger, J.P., Millan-Gabet, R., & Ten Brummelaar, T.A. 2004, in New Frontiers in Stellar Interferometry, Proc. SPIE, 5491, ed. W.A. Traub, p.1370

Morgan, R.M., Burge, J., & Woolf, N. 2000, "Nulling Interferometric Beam Combiner Utilizing Dielectric Plates: Experimental Results in the Visible Broadband, in Interferometry in Optical Astronomy", eds. P.J. Lena & A. Quirrenbach, SPIE Vol. 4006, p. 340

Mozurkewich, D. 1994, "A Hybrid Design for a Six Way Beam Combiner", SPIE 2200, p. 76

Pancharatnam, S. 1955, "Achromatic Combinations of Birefringent Plates. Part I. An Achromatic Circular Polarizer, and Part II. An Achromatic Quarter-Wave Plate", Proc. Ind. Acad. Sci., XLI, No.4, Sec. A, 130-144

Peyrilloux, A., Pagnoux, D., & Reynaud, F. 2003, "Evaluation of Photonic Crystal Fiber Potential for Fiber Linked Version of Stellar Interferometers", SPIE 4838, p. 1334

Reynaud, F. & Delaire, E. 1994, "Linear Optical Path Modulation with a lambda/200 Accuracy Using a Fiber Stretcher", Proc. SPIE 2209, p. 501

Ridgeway, S.T. 1994, "Infrared Beam Combining and Detection", CHARA technical memo, No. L

Serkowsky, K. 1974, Methods of Experimental PhysicsVol 12: Astrophysics, Part A, N. P. Carleton, Hrsg, (1974), p.361

Shao, M. & Colavita, 1992. "Long-baseline Optical and Stellar Interferometry", ARAA, 30, 457

Ten Brummelaar, T. 1994, "Visible Light Imaging", CHARA technical memo, No. K

Ten Brummelaar, T. 1995, "Correlation Measurement and Group Delay Tracking with a Noisy Detector", CHARA Technical Report No. 24,

Wyant, J.C. 1975, "Use of an AC Heterodyne Lateral Shear Interferometer with Real-Time Wavefront Correction Systems", Appl. Opt. 14, 2622

Zhang, X. 2002, "Atmospheric Differential Refraction Correction on NPOI", NPOI technical memorandum